ANZIAM J. 54(2013), 181–199
doi:10.1017/S1446181113000138

AN IMPROVED SECOND-ORDER NUMERICAL METHOD FOR THE GENERALIZED BURGERS–FISHER EQUATION

A. G. BRATSOS[1]

(Received 16 February, 2011; revised 30 January, 2013; first published online 12 June, 2013)

Abstract

A second-order in time finite-difference scheme using a modified predictor–corrector method is proposed for the numerical solution of the generalized Burgers–Fisher equation. The method introduced, which, in contrast to the classical predictor–corrector method is direct and uses updated values for the evaluation of the components of the unknown vector, is also analysed for stability. Its efficiency is tested for a single-kink wave by comparing experimental results with others selected from the available literature. Moreover, comparisons with the classical method and relevant analogous modified methods are given. Finally, the behaviour and physical meaning of the two-kink wave arising from the collision of two single-kink waves are examined.

2010 *Mathematics subject classification*: primary 35K57; secondary 35Q51, 65M06, 65Y10.

Keywords and phrases: generalized Burgers–Fisher equation, reaction–diffusion equation, finite-difference method, bistable medium, travelling kink waves, modified predictor–corrector method.

1. Introduction

In 1937, R. A. Fisher [13] devised the equation

$$u_t - u_{xx} = u(1 - u),$$

known thenceforth as the Fisher equation, for the simulation of the propagation of a gene in a population. In the same year, Kolmogorov et al. [20] independently devised the same equation to describe the dynamic spread of a combustion front. For this reason, the names Fisher–Kolmogorov and Fisher–KPP are also used for this equation. The Fisher equation is a prototypical reaction–diffusion equation with a quadratic reactive term corresponding to logistic growth, and its theoretical solution was first given by Ablowitz and Zeppetella [1] in 1979. Since then, the mathematical

[1]Department of Mathematics, Technological Educational Institution (TEI) of Athens, 122 10 Egaleo, Athens, Greece; e-mail: bratsos@teiath.gr. URL: http://users.teiath.gr/bratsos/.

properties of the Fisher equation have been extensively studied; there have been numerous discussions in the literature and it has been mentioned in numerous contexts, describing heat and mass transfer, combustion theory, biology and ecology (see, for example, the paper by Brazhnik and Tyson [26] and references therein). A summary of numerical methods is given by Zhao et al. [32].

The most general form of the Fisher equation is the so-called generalized Burgers–Fisher equation. The (1 + 1)-dimensional generalized Burgers–Fisher (BgF) equation, which is examined here, has the form

$$u_t + \alpha u^{\delta} u_x - u_{xx} = \beta u(1 - u^{\delta}), \quad 0 \le x \le 1, t > 0, \tag{1.1}$$

with initial condition

$$u(x, 0) = f(x), \quad 0 \le x \le 1, \tag{1.2}$$

and boundary conditions

$$u_x|_{x=0,1} = 0, \quad t > 0. \tag{1.3}$$

Here, the real-valued function $u = u(x, t)$ is a sufficiently differentiable function of the space and time variables; α, β are real parameters and δ is a positive integer. It is straightforwardly derived from equation (1.1) that, in general, the medium described by u has the property of being a bistable one, since it has two homogeneous stationary states, $u = 0$ and $u = 1$. When $\beta = 0$, equation (1.1) is the modified Burgers equation (see our earlier paper [8] and references therein); when $\alpha = 0$, equation (1.1) is the generalized Fisher equation and its theoretical solution is given by Wang [27] and Wazwaz [28].

It is known [28] that equation (1.1) has the following single-kink solution:

$$u(x, t) = \left\{\tfrac{1}{2} + \tfrac{1}{2}\tanh[k(x - ct)]\right\}^{1/\delta}, \tag{1.4}$$

in which

$$k = -\frac{\alpha\delta}{2(\delta + 1)} \quad \text{and} \quad c = \frac{\alpha}{\delta + 1} + \frac{\beta(\delta + 1)}{\alpha}$$

are the wave number and the velocity, respectively. Because of the aforementioned bistable property of u, this kink-like travelling wave solution describes a constant-velocity front of transition from one homogeneous state to another (see Proposition A.1). Then a two-kink wave solution is given by

$$u(x, t) = \sum_{i=1}^{2} q_i \left\{\frac{1}{2} + \frac{1}{2}\tanh[k_i(x - c_i t)]\right\}^{1/\delta_i}, \tag{1.5}$$

where q_i is either $+1$ or -1; and k_i, c_i and δ_i, for $i = 1, 2$, are the wave number, the velocity and the theoretical parameter corresponding to the i-kink, respectively. Subject again to the aforementioned bistable property of the BgF equation, the solution (1.5), in general, describes a constant-velocity front of transition from $-1 + \varepsilon$ to $1 - \tilde{\varepsilon}$

https://doi.org/10.1017/S1446181113000138 Published online by Cambridge University Press

or from $0 \pm \varepsilon$ to $\pm 2 \pm \tilde{\varepsilon}$ with $\varepsilon, \tilde{\varepsilon} \in [\,0, 1]$ depending on the values of the signs of q_i and c_i, $i = 1, 2$ (see Proposition A.2).

Equation (1.1) has a wide range of applications in plasma physics, fluid physics, capillary–gravity waves, nonlinear optics and chemical physics. Many researchers have studied it theoretically and numerically. Because of its strong nonlinearity, it is often used as a model problem to test various numerical methods, where, among others, finite-difference methods [16, 23, 24], the Adomian decomposition method [17, 19] and differential quadrature [22] have been used. Powerful mathematical methods such as the tanh [11, 28], extended tanh [10], tanh–coth [29, 30], exp-function [31], variational iteration [21], homotopy analysis [2], factorization [12] and spectral collocation [14, 18] methods have also been used for this equation.

The main aim of this paper is to solve the BgF equation with a direct and explicit method. For this purpose, and usually because the real-world problem of minimizing the calculations required in a numerical method is one of the necessary components for the accuracy of the results achieved, a second-order in time numerical method analogous to that in our earlier paper [4] is used. In the resulting nonlinear system, the solution is given directly by expressing the unknown vector explicitly, and then, considering the vector componentwise during the evaluation process, the unknown components are updated with the known values. This process, which is known as a modified predictor–corrector (MPC) method, in contrast to the iterative classical predictor–corrector (PC) method, is always *explicit* and is applied *once*. It has also been applied successfully with second-, third- and fourth-order in time approximations in other nonlinear partial differential equations (PDEs) [3–9], giving an improvement in the accuracy over the PC method. Owing to the need to minimize the calculations mentioned above, the order of the approximation used for this process will always be a subject of research. The results from the experiments in this paper are analysed and compared with the known results for the BgF equation, and conclusions for the efficiency of the MPC over the PC method and comparisons with the other MPC methods mentioned are given. Also, the behaviour of a two-kink wave arising from the collision of two single-kink waves is examined.

The paper is organized as follows. In Section 2, the proposed nonlinear method arising from equation (1.1) by using finite-difference approximations analogous to those used previously [8] is defined and its stability is investigated. The predictor and the MPC method are defined and developed in Section 3. Extensive numerical results concerning both the single-kink wave and the collision of two single-kink waves are reported in Section 4 to facilitate the understanding of the efficiency of the method introduced for the numerical solution of equation (1.1), and detailed comparisons with the aforementioned category of MPC methods are given. Some conclusions are drawn in Section 5.

2. Numerical method

2.1. Grid and solution vector Consider the region $R = \{(x, t) \in [0, 1] \times (0, T]\}$ with its boundary ∂R consisting of the lines $x = 0$, $x = 1$ and $t = 0$, covered with a

https://doi.org/10.1017/S1446181113000138 Published online by Cambridge University Press

rectangular mesh of points G with coordinates $(x,t)=(x_m,t_n)=(mh,n\ell)$ with $n=1,2,\ldots$ and $m=0,1,\ldots,N+1$. The theoretical solution of equation (1.1) at the typical mesh point (x_m,t_n) is denoted by u_m^n, while that relevant to an approximating difference scheme is denoted by U_m^n.

Let the solution vector at time level $t=t_n$ be

$$\mathbf{U}^n=\mathbf{U}(t_n)=[U_0^n,U_1^n,\ldots,U_{N+1}^n]^\top.$$

2.2. Nonlinear system Using for the space derivatives analogous approximations to those in our previous paper [8], equation (1.3) in the second-order approximation gives $U_{-1}^n=U_1^n$ and $U_{N+2}^n=U_N^n$. Applying equation (1.1) at each point of the grid G at time level $t=t_n=n\ell$, $n=1,2,\ldots$, we use for the first-order space derivative the usual central-difference approximant at each point of (0, 1) and the forward one at $x=0,1$; for the second-order space derivative, the second-order central-difference approximant is used. This leads to a first-order initial-value problem written in a matrix–vector form as

$$\begin{aligned} D\mathbf{U}(t)&=-\alpha\Delta A\mathbf{U}(t)+B\mathbf{U}(t)+\beta\tilde{\Delta}\mathbf{U}(t),\quad t>0,\\ \mathbf{U}^0&=\mathbf{U}(0)=[f(x_0),f(x_1),\ldots,f(x_{N+1})]^\top=\mathbf{f}, \end{aligned}\tag{2.1}$$

in which $D=\operatorname{diag}\{d/dt\}$ is the first-order differential operator;

$$\Delta=\Delta(t)=\Delta^n=\operatorname{diag}\{\Delta_m^n\}=\operatorname{diag}\{(U_m^n)^\delta\},\tag{2.2}$$

$$\tilde{\Delta}=\tilde{\Delta}(t)=\tilde{\Delta}^n=\operatorname{diag}\{\tilde{\Delta}_m^n\}=\operatorname{diag}\{1-(U_m^n)^\delta\},\tag{2.3}$$

for $n=1,2,\ldots$ and $m=0,1,\ldots,N+1$ are diagonal matrices;

$$A=\frac{1}{2h}\begin{bmatrix} -2 & 2 & & & \\ -1 & 0 & 1 & & \\ & \ddots & \ddots & \ddots & \\ & & -1 & 0 & 1\\ & & & 2 & -2 \end{bmatrix},\quad B=\frac{1}{h^2}\begin{bmatrix} -2 & 2 & & & \\ 1 & -2 & 1 & & \\ & \ddots & \ddots & \ddots & \\ & & 1 & -2 & 1\\ & & & 2 & -2 \end{bmatrix}$$

are tridiagonal matrices; and $\mathbf{f}=[f_0,f_1,\ldots,f_{N+1}]^\top$ is the vector of the initial condition, all of order $N+2$.

Equation (2.1) leads to the following expression for the operator D related to the BgF equation:

$$D=-\alpha\Delta A+B+\beta\tilde{\Delta}.\tag{2.4}$$

Using the recurrence relation

$$\mathbf{U}(t+\ell)=\exp(\ell D)\mathbf{U}(t),\quad t=0,\ell,\ldots,$$

where D is given by (2.4), and replacing $\exp(\ell D)$ with the second-order rational replacements [25, p. 134] of the form

$$(I-\tfrac{1}{2}\ell D)\mathbf{U}(t+\ell)=(I+\tfrac{1}{2}\ell D)\mathbf{U}(t),\tag{2.5}$$

https://doi.org/10.1017/S1446181113000138 Published online by Cambridge University Press

and using the notation of (2.2)–(2.3) and equation (2.4), we obtain the following nonlinear system:

$$\begin{aligned}\mathbf{U}(t+\ell) - \tfrac{1}{2}\ell(-\alpha\Delta^{n+1}A + B + \beta\tilde{\Delta}^{n+1})\mathbf{U}(t+\ell)\\ = \mathbf{U}(t) + \tfrac{1}{2}\ell(-\alpha\Delta^{n}A + B + \beta\tilde{\Delta}^{n})\mathbf{U}(t).\end{aligned} \tag{2.6}$$

Let $r_1 = \ell\alpha/4\,h$, $r_2 = \ell/2\,h^2$ and $r_3 = \ell\beta/2$. Equation (2.6) subject to the boundary condition (1.3) and the notation of (2.2)–(2.3), when applied to a general mesh point of the grid G, gives

$$\begin{aligned}U_m^{n+1} + r_1\Delta_m^{n+1}(-U_{m-1}^{n+1} + U_{m+1}^{n+1}) - r_2(U_{m-1}^{n+1} - 2U_m^{n+1} + U_{m+1}^{n+1}) - r_3\tilde{\Delta}_m^{n+1}U_m^{n+1}\\ = U_m^n - r_1\Delta_m^n(-U_{m-1}^n + U_{m+1}^n) + r_2(U_{m-1}^n - 2U_m^n + U_{m+1}^n) + r_3\tilde{\Delta}_m^n U_m^n\end{aligned} \tag{2.7}$$

for $m = 0, 1, \ldots, N+1$.

2.2.1. Stability analysis Following the Fourier method of analysing stability [25, p. 142], if $\xi = e^{\alpha\ell}$ is the amplification factor and $\tilde{U}_m^n$ the numerical value of U_m^n actually obtained, an error of the form $U_m^n - \tilde{U}_m^n = \xi^n e^{im\beta h}$, where $i = \sqrt{-1}$ with α a complex number and β real, is considered. Equation (2.7) leads to the following stability equation:

$$\begin{aligned}[1 - r_1\tilde{\Delta}_0 + 4r_3\sin^2\omega + 2ir_2\Delta_0\sin 2\omega]\xi\\ = 1 + 2r_1\tilde{\Delta}_0 - 8r_3\sin^2\omega - 4i\Delta_0 r_2\sin 2\omega,\end{aligned} \tag{2.8}$$

where $\Delta_0 = U_0^\delta$, $\tilde{\Delta}_0 = 1 - U_0^\delta$ with U_0 a typical value of U_m^{n+1}, U_m^n, $m = 0, 1, \ldots, N+1$ used for the linearization of the nonlinear terms of equation (2.7), and $\omega = \beta h/2$ with $\omega \in [0, \pi/2]$. Equation (2.8) is of the form

$$\breve{A}\xi = \breve{B}, \quad \breve{A}, \breve{B} \in C,$$

with C the set of the complex numbers, so the von Neumann necessary criterion for stability $|\xi| \le 1$ will always be satisfied when

$$|\breve{B}| \le |\breve{A}|. \tag{2.9}$$

For $\omega = 0$, inequality (2.9) leads to

$$|1 + 2r_1\tilde{\Delta}_0| \le |1 - r_1\tilde{\Delta}_0|,$$

which holds for $\beta = 0$, and for $\beta \neq 0$ is satisfied when

$$\ell \ll 1. \tag{2.10}$$

If $\omega = \pi/2$, (2.9) leads to $|1 + 2r_1\tilde{\Delta}_0 - 8r_3| \le |1 + 4r_3 - r_1\tilde{\Delta}_0|$, which holds, since subject to inequality (2.10) the terms $r_1\tilde{\Delta}_0$ and r_3 can be omitted.

https://doi.org/10.1017/S1446181113000138 Published online by Cambridge University Press

3. Modified predictor–corrector method

The nonlinear system (2.6) is solved by a direct process in the following.

3.1. Predictor The value $\hat{\mathbf{U}}(t+\ell)$ is evaluated using the Maclaurin expansion

$$\mathbf{U}(t+\ell) = (I + \ell D + \tfrac{1}{2}\ell^2 D^2)\mathbf{U}(t) + O(\ell^3) \quad \text{as } \ell \to 0. \tag{3.1}$$

Equation (3.1), using the notation of (2.2)–(2.3) and subject to (2.4), leads to

$$\begin{aligned}\hat{\mathbf{U}}(t+\ell) =& \mathbf{U}(t) + \ell[-\alpha\Delta^n A + B + \beta\tilde{\Delta}^n]\mathbf{U}(t)\\ &+ \frac{\ell^2}{2}[(\alpha\Delta^n A)^2 + B^2 + (\beta^2\tilde{\Delta}^n)^2 - \alpha\Delta^n AB - \alpha\beta\Delta^n A\tilde{\Delta}^n\\ &- \alpha B\Delta^n A + \beta B\tilde{\Delta}^n - \alpha\beta\tilde{\Delta}^n\Delta^n A + \beta\tilde{\Delta}^n B]\mathbf{U}(t).\end{aligned} \tag{3.2}$$

Let $p_1 = \ell/h^2$, $p_2 = \ell\alpha/2\,h$, $p_3 = \ell^2\alpha^2/8\,h^2$, $p_4 = \ell^2\beta^2/2$, $p_5 = \ell^2/2\,h^4$, $p_6 = \ell^2\alpha/4\,h^3$, $p_7 = \ell^2\alpha\beta/4\,h$ and $p_8 = \ell^2\beta/2\,h^2$. Equation (3.2), subject again to the boundary condition (1.3), when applied to the general mesh point of the grid G, gives

$$\begin{aligned}\hat{U}_m^{n+1} =& U_m^n + \ell\beta\tilde{\Delta}_m^n U_m^n + p_1(U_{m-1}^n - 2U_m^n + U_{m+1}^n) - p_2\Delta_m^n(U_{m+1}^n - U_{m-1}^n)\\ &+ p_3\Delta_m^n[\Delta_{m-1}^n U_{m-2}^n - (\Delta_{m-1}^n + \Delta_{m+1}^n)U_m^n + \Delta_{m+1}^n U_{m+2}^n]\\ &+ p_4(\tilde{\Delta}_m^n)^2 U_m^n + p_5(U_{m-2}^n - 4U_{m-1}^n + 6U_m^n - 4U_{m+1}^n + U_{m+2}^n)\\ &- p_6\Delta_m^n[-U_{m-2}^n + 2(U_{m-1}^n - U_{m+1}^n) + U_{m+2}^n]\\ &- p_7\Delta_m^n(\tilde{\Delta}_{m+1}^n U_{m+1}^n - \tilde{\Delta}_{m-1}^n U_{m-1}^n)\\ &- p_6[-\Delta_{m-1}^n U_{m-2}^n + 2\Delta_m^n(U_{m-1}^n - U_{m+1}^n) + (\Delta_{m-1}^n - \Delta_{m+1}^n)U_m^n + \Delta_{m+1}^n U_{m+2}^n]\\ &+ p_8(\tilde{\Delta}_{m-1}^n U_{m-1}^n - 2\tilde{\Delta}_m^n U_m^n + \tilde{\Delta}_{m+1}^n U_{m+1}^n)\\ &- p_7\Delta_m^n\tilde{\Delta}_m^n(U_{m+1}^n - U_{m-1}^n) + p_8\tilde{\Delta}_m^n(U_{m-1}^n - 2U_m^n + U_{m+1}^n)\end{aligned} \tag{3.3}$$

for $m = 0, 1, \ldots, N+1$.

3.1.1. Stability analysis Following again the Fourier method of analysing stability, equation (3.3) leads to the following stability equation:

$$\begin{aligned}\xi =& 1 + \ell\beta\tilde{\Delta}_0 + p_4\tilde{\Delta}_0^2 - 4(p_1 + 2p_8\tilde{\Delta}_0)\sin^2\omega + 16p_5\sin^4\omega - 4p_3\Delta_0^2\sin^2 2\omega\\ &+ 2i\Delta_0[(-p_2 + 4p_6 - 2p_7\tilde{\Delta}_0)\sin 2\omega - 4p_6\sin 4\omega]\\ =& K(\omega) + i\Lambda(\omega).\end{aligned}$$

Then the von Neumann necessary criterion for stability $|\xi| \le 1$ gives

$$\sqrt{K^2(\omega) + \Lambda^2(\omega)} \le 1. \tag{3.4}$$

If $\omega = 0$, inequality (3.4) leads to

$$|1 + \ell\beta\tilde{\Delta}_0 + \tfrac{1}{2}\ell^2\beta^2\tilde{\Delta}_0^2| \le 1,$$

which for $\beta = 0$ is trivial, and for $\beta \ne 0$ is satisfied when condition (2.10) holds.

https://doi.org/10.1017/S1446181113000138 Published online by Cambridge University Press

If $\omega = \pi/2$, inequality (3.4) leads to

$$\left|1 + \left(-\frac{4}{h^2} + \beta\tilde{\Delta}_0\right)\ell + \left(\frac{8}{h^4} - \frac{4}{h^2}\beta\tilde{\Delta}_0 + \frac{1}{2}\beta^2\tilde{\Delta}_0^2\right)\ell^2\right| \le 1,$$

which is satisfied when

$$\left(-\frac{4}{h^2} + \beta\,\tilde{\Delta}_0\right)\ell + \left(\frac{8}{h^4} - \frac{4}{h^2}\beta\tilde{\Delta}_0 + \frac{1}{2}\beta^2\tilde{\Delta}_0^2\right)\ell^2 \le 0. \tag{3.5}$$

For $\beta = 0$, inequality (3.5) leads to the following restriction for the time step:

$$\ell \le \frac{h^2}{2}. \tag{3.6}$$

For $\beta \neq 0$, provided that for the space step the inequality

$$h < 2|\beta\tilde{\Delta}_0|^{-1/2}$$

holds, (3.5) leads to $\ell \le 2h^2/(4 - h^2\beta\tilde{\Delta}_0)^{-1}$. The latter inequality, which, using Maclaurin's expansion of the right-hand side, is written as

$$\ell \le \frac{h^2}{2} + \frac{1}{8}\beta\tilde{\Delta}_0 h^4 + O(h^6),$$

leads to the following restriction for the time step:

$$\ell \le \frac{h^2}{2} + \frac{1}{8}\beta\tilde{\Delta}_0 h^4. \tag{3.7}$$

Subject to (2.10), the more restrictive of the inequalities (3.6) and (3.7) is used for our experiments.

3.2. Corrector The corrector used for the MPC method arises from equation (2.5) as follows:

$$\mathbf{U}(t+\ell) = \tfrac{1}{2}\ell D\hat{\mathbf{U}}(t+\ell) + (I + \tfrac{1}{2}\ell D)\mathbf{U}(t). \tag{3.8}$$

Considering equation (3.8) componentwise and using the updated component in the corrector vector as soon as it becomes available leads to

$$\begin{aligned} U_m^{n+1} &= -r_1\hat{\Delta}_m^{n+1}(-U_{m-1}^{n+1} + \hat{U}_{m+1}^{n+1}) + r_2(U_{m-1}^{n+1} - 2\hat{U}_m^{n+1} + \hat{U}_{m+1}^{n+1}) + r_3\breve{\Delta}_m^{n+1}U_m^{n+1} \\ &= U_m^n - r_1\Delta_m^n(-U_{m-1}^n + U_{m+1}^n) + r_2(U_{m-1}^n - 2U_m^n + U_{m+1}^n) + r_3\tilde{\Delta}_m^n U_m^n \end{aligned}$$

for $m = 0, 1, \ldots, N+1$, where, following the notation of (2.2)–(2.3),

$$\begin{aligned} \hat{\Delta} &= \hat{\Delta}(t+\ell) = \hat{\Delta}^{n+1} = \mathrm{diag}\{\hat{\Delta}_m^{n+1}\} = \mathrm{diag}\{(\hat{U}_m^{n+1})^\delta\}, \\ \breve{\Delta} &= \breve{\Delta}(t+\ell) = \breve{\Delta}^{n+1} = \mathrm{diag}\{\breve{\Delta}_m^{n+1}\} = \mathrm{diag}\{1 - (\hat{U}_m^{n+1})^\delta\}. \end{aligned}$$

See Section 2.2.1 for the stability analysis of the corrector.

https://doi.org/10.1017/S1446181113000138 Published online by Cambridge University Press

4. Numerical results

The accuracy of our method is measured by computing the root mean square and maximum norms by using differences between the analytical and numerical results at the node points, by way of calculation of the discrete L_2 and L_∞ error norms defined by

$$L_2 = \left(h \sum_{m=0}^{N+1} |u_m^n - U_m^n|^2 \right)^{1/2}, \quad L_\infty = \max_{m=0,1,\ldots,N+1} |u_m^n - U_m^n|.$$

Let x_e denote the x-coordinate of the point at which L_∞ occurs. In all experiments, for the linearization term U_0 defined in equation (2.8), the value $U_0 = \max_{m=0,1,\ldots,N+1}\{u_m^0\}$ was given.

4.1. Single-kink wave In all experiments, the initial condition (1.2) was given by the value $f(x) = u(x, 0)$, with u the theoretical solution (1.4). Experiments showed that the most accurate results are obtained for $h \in [0.05, 0.1]$ and $\ell \leq 10^{-3}$.

4.1.1. Accuracy of the method The accuracy of the MPC method for the numerical solution of the BgF equation is examined by comparing the results from the experiments with selected existing relevant results [17, 19, 21, 23] using the same Dirichlet boundary conditions,

$$U_0^n = u(0, t) \quad \text{and} \quad U_{N+1}^n = u(1, t), \quad t > 0,$$

together with (1.3) and theoretical parameter values. Also, in order for the comparison with the known relevant time levels to be possible, the value $\ell = 10^{-4}$ is used. From the numerical results given in Tables 1–5 and additional results not shown for the sake of brevity, the following conclusions for the MPC method are drawn.

Problem I [17] When $\beta \neq 0$, the method gives more accurate results for all time levels and δ used than the relevant results of Ismail et al. [17] and Sari [23] using the Adomian decomposition and a finite-difference method, respectively (see Table 1), and of Ismail et al. [17] for $\beta = 0$ (Table 2). Also, in the latter table, as δ and t increase, a convergence of the numerical and the theoretical solutions appears.

Problem II [19] More accurate results are derived for all time levels and δ used than the relevant results of Sari [23] (Table 3) and Kaya and El-Sayed [19] using the Adomian decomposition method (Table 4). In the same way as in Problem I, a convergence of the numerical and theoretical solutions appears as time increases.

Problem III [21] Finally, the method was compared to a selected example of Moghimi and Hejazi [21, p. 1759], where the variational iteration method was used, with $\delta = 1$, $\alpha = 0.01$ and $\beta = 0.01$. It is seen from Table 5 that the results are more accurate than those of Moghimi and Hejazi [21], and as was found in Problems I and II, a convergence with the theoretical solution occurs for long time periods.

https://doi.org/10.1017/S1446181113000138 Published online by Cambridge University Press

Table 1. Problem I [17]. Comparisons for various values of x, t and δ (and $h = 0.1$, $\ell = 10^{-4}$).

		$\alpha=\beta=0.001$		$\delta=1$			$\delta=4$	
t	x	Theoretical	Method	L_∞	L_∞ [17]	L_∞ [23]	L_∞	L_∞ [23]
0.001	0.1	0.4999878	0.4999878	1.15×10^{-10}	1.94×10^{-6}	1.01×10^{-7}	7.71×10^{-11}	1.75×10^{-8}
	0.5	0.4999378	0.4999378	3.05×10^{-13}	1.94×10^{-6}	1.04×10^{-7}	2.06×10^{-13}	1.75×10^{-8}
	0.9	0.4998878	0.4998877	1.12×10^{-10}	1.94×10^{-6}	1.01×10^{-7}	7.57×10^{-11}	1.75×10^{-8}
0.010	0.1	0.4999900	0.4999900	6.01×10^{-10}	1.94×10^{-5}	7.53×10^{-7}	4.04×10^{-10}	1.27×10^{-6}
	0.5	0.4999400	0.4999400	5.59×10^{-12}	1.94×10^{-5}	1.04×10^{-6}	3.76×10^{-12}	1.75×10^{-6}
	0.9	0.4998900	0.4998900	4.97×10^{-10}	1.94×10^{-5}	7.53×10^{-7}	3.34×10^{-10}	1.27×10^{-6}
		$\alpha=\beta=1$		$\delta=2$				$\delta=8$
0.0005	0.1	0.6954258	0.6954258	5.46×10^{-8}	1.40×10^{-3}	7.62×10^{-5}	2.47×10^{-8}	1.02×10^{-4}
	0.5	0.6462972	0.6462972	5.79×10^{-9}	1.35×10^{-3}	9.14×10^{-5}	3.04×10^{-11}	1.37×10^{-4}
	0.9	0.5954813	0.5954812	6.48×10^{-8}	1.28×10^{-3}	1.02×10^{-4}	3.28×10^{-8}	1.69×10^{-4}
0.0010	0.1	0.6956252	0.6956253	1.04×10^{-7}	2.80×10^{-3}	1.50×10^{-4}	5.22×10^{-8}	2.00×10^{-4}
	0.5	0.6465062	0.6465062	1.15×10^{-8}	2.69×10^{-3}	1.83×10^{-4}	2.14×10^{-11}	2.74×10^{-4}
	0.9	0.5956948	0.5956947	1.23×10^{-7}	2.55×10^{-3}	2.00×10^{-4}	6.18×10^{-8}	3.31×10^{-4}

Table 2. Problem I [17]. Comparisons and other results for various values of x, t and δ with $\alpha = 1$ and $\beta = 0$ (and $h = 0.1$, $\ell = 10^{-4}$).

δ	t	x	Theoretical	Method	L_∞	L_∞ [17]	t	L_∞
1	2	0.1	0.6106392	0.6106399	6.92×10^{-7}	6.43×10^{-5}	20	7.90×10^{-8}
		0.5	0.5621765	0.5621758	6.58×10^{-7}	6.07×10^{-5}		1.81×10^{-7}
		0.9	0.5124974	0.5124964	9.86×10^{-7}	4.75×10^{-5}		5.14×10^{-8}
2	2	0.1	0.7702837	0.7702846	8.61×10^{-7}	1.19×10^{-5}	20	1.28×10^{-7}
		0.5	0.7264635	0.7264636	9.12×10^{-8}	1.50×10^{-5}		3.37×10^{-7}
		0.9	0.6791092	0.6791085	7.21×10^{-7}	1.44×10^{-5}		1.13×10^{-7}
3	0.001	0.1	0.7836828	0.7836829	9.16×10^{-8}	4.44×10^{-4}	10	8.58×10^{-7}
		0.5	0.7413093	0.7413093	6.75×10^{-9}	1.85×10^{-3}		1.97×10^{-6}
		0.9	0.6961834	0.6961833	1.09×10^{-7}	9.05×10^{-4}		5.14×10^{-7}
8	4	0.1	0.9333578	0.9333585	6.52×10^{-7}		40	9.88×10^{-8}
		0.5	0.9141433	0.9141442	8.60×10^{-7}			2.91×10^{-7}
		0.9	0.8918148	0.8918147	6.43×10^{-8}			1.09×10^{-7}

Table 3. Problem II [19]. Comparisons of the proposed method for various values of x, t and δ with $\alpha = 0.1$ and $\beta = -0.0025$ (and $h = 0.1$, $\ell = 10^{-4}$).

		$\delta=2$			$\delta=4$			$\delta=8$
t	x	Theoretical	L_∞	L_∞ [23]	L_∞	L_∞ [23]	L_∞	L_∞ [23]
0.1	0.1	0.7058781	9.85×10^{-8}	1.21×10^{-5}	7.03×10^{-8}	1.34×10^{-5}	4.26×10^{-8}	1.47×10^{-5}
	0.5	0.7011405	3.30×10^{-8}	2.90×10^{-5}	2.36×10^{-8}	3.49×10^{-5}	1.44×10^{-8}	3.83×10^{-5}
	0.9	0.6963728	5.58×10^{-8}	1.54×10^{-5}	4.04×10^{-8}	1.39×10^{-5}	2.47×10^{-8}	1.53×10^{-5}
0.3	0.1	0.7057797	1.06×10^{-7}	1.60×10^{-5}	7.59×10^{-8}	1.92×10^{-5}	4.61×10^{-8}	2.11×10^{-5}
	0.5	0.7010415	5.65×10^{-8}	4.47×10^{-5}	4.04×10^{-8}	5.37×10^{-5}	2.46×10^{-8}	5.91×10^{-5}
	0.9	0.6962732	4.91×10^{-8}	1.64×10^{-5}	3.56×10^{-8}	1.98×10^{-5}	2.18×10^{-8}	2.18×10^{-5}
0.5	0.1	0.7056813	1.07×10^{-7}	1.67×10^{-5}	7.67×10^{-8}	2.00×10^{-5}	4.66×10^{-8}	2.20×10^{-5}
	0.5	0.7009424	5.98×10^{-8}	4.69×10^{-5}	4.28×10^{-8}	5.64×10^{-5}	2.60×10^{-8}	6.22×10^{-5}
	0.9	0.6961735	4.81×10^{-8}	1.71×10^{-5}	3.49×10^{-8}	2.07×10^{-5}	2.14×10^{-8}	2.28×10^{-5}
2.0	0.1	0.7049429	1.08×10^{-7}		7.71×10^{-8}		4.72×10^{-8}	
	0.5	0.7001993	6.04×10^{-8}		4.34×10^{-8}		2.66×10^{-8}	
	0.9	0.6954258	4.80×10^{-8}		3.49×10^{-8}		2.16×10^{-8}	

https://doi.org/10.1017/S1446181113000138 Published online by Cambridge University Press

TABLE 4. Problem II [19]. Comparisons of the proposed method for various values of x and δ with $\alpha = 0.1$ and $\beta = -0.0025$ (and $h = 0.1$, $\ell = 10^{-4}$).

		$\delta = 2$		$\delta = 4$		$\delta = 6$		$\delta = 8$	
t	x	L_∞	L_∞ [19]	L_∞	L_∞ [19]	L_∞	L_∞ [19]	L_∞	L_∞ [19]
0.5	0.1	1.07×10^{-7}	6.10×10^{-6}	7.67×10^{-8}	7.35×10^{-5}	5.81×10^{-8}	1.08×10^{-5}	4.66×10^{-8}	1.20×10^{-5}
	0.5	5.98×10^{-8}	3.07×10^{-5}	4.28×10^{-8}	3.68×10^{-5}	3.25×10^{-8}	5.38×10^{-5}	2.60×10^{-8}	5.97×10^{-5}
5.0	0.1	1.08×10^{-7}		7.79×10^{-8}		5.97×10^{-8}		4.84×10^{-8}	
	0.5	6.05×10^{-8}		4.38×10^{-8}		3.36×10^{-8}		2.72×10^{-8}	

TABLE 5. Problem III [21]. Comparisons and other results of the proposed method for various values of x and t with $\delta = 1$, $\alpha = 0.01$ and $\beta = 0.01$ (and $h = 0.1$, $\ell = 10^{-4}$).

	$t = 1$			$t = 10$		$t = 50$	
x	Theoretical	L_∞	L_∞ [21]	L_∞	L_∞ [21]	L_∞	L_∞ [21]
0.1	0.5023812	1.14×10^{-8}	1.78×10^{-8}	1.13×10^{-8}	2.07×10^{-5}	1.07×10^{-8}	0.002552
0.5	0.5018812	6.33×10^{-9}	5.29×10^{-9}	6.32×10^{-9}	1.94×10^{-5}	5.96×10^{-9}	0.002522
0.9	0.5013812	5.04×10^{-9}	7.28×10^{-9}	5.03×10^{-9}	1.81×10^{-5}	4.75×10^{-9}	0.002492
	$t = 100$			$t = 200$		$t = 300$	
	Theoretical	Method	L_∞	Theoretical	L_∞	Theoretical	L_∞
0.1	0.7314516	0.7314516	8.93×10^{-9}	0.8812687	4.76×10^{-9}	0.9528894	2.04×10^{-9}
0.5	0.7310586	0.7310586	4.98×10^{-9}	0.8810593	2.65×10^{-9}	0.9527995	1.14×10^{-9}
0.9	0.7306652	0.7306652	3.97×10^{-9}	0.8808496	2.12×10^{-9}	0.9527095	9.09×10^{-10}

4.1.2. Efficiency of the method The efficiency of the MPC method over the standard PC method is investigated in the following. Let

$$\rho(t) = \frac{L_\infty^{\mathrm{PC}}}{L_\infty^{\mathrm{MPC}}} \quad \text{and} \quad \tilde{\rho}(t) = \frac{L_2^{\mathrm{PC}}}{L_2^{\mathrm{MPC}}}$$

denote the ratios of the average errors at selected time levels t with $t \in (0, T]$ using the PC and the MPC methods for both the error norms L_∞ and L_2.

BgF equation: comparison of the MPC method with the PC method In contrast to the boundary conditions and time levels used in Section 4.1.1, the boundary condition (1.3) and long time periods often appearing in real-world problems were used. From the results given in Table 6, the following are deduced:

- The MPC method gives more accurate results than the PC method for both the error norms L_∞ and L_2 at all time steps and levels examined.
- When the time step is refined, the MPC method still gives an improvement in accuracy over the PC methods, but this improvement becomes insignificant [5, p. 276].

BgF equation: comparisons with known MPC methods The MPC method has already been used in the numerical solution of the nonlinear sine-Gordon equations in one (Sg1) [7] and two (Sg2) [3, 5, 6] dimensions, Boussinesq (Bq) [4], Schrödinger (NLS) [9] and modified Burgers (MBg) [8] equations. Selected results comparing the

https://doi.org/10.1017/S1446181113000138 Published online by Cambridge University Press

Table 6. Comparisons of the MPC and PC methods for the BgF equation (for $h = 0.1$).

Problem	ℓ	t	Method	L_∞	L_2
[17] $\delta = 1$	10^{-3}	1	MPC	0.6251571×10^{-4}	0.4592807×10^{-4}
$\alpha = 0.001$			PC	0.6255543×10^{-4}	0.4593336×10^{-4}
$\beta = 0.001$		10	MPC	0.6307926×10^{-4}	0.4601020×10^{-4}
			PC	0.6311830×10^{-4}	0.4601612×10^{-4}
	10^{-3}	10		$\rho(10) = 1.000627$	$\tilde{\rho}(10) = 1.000122$
	10^{-4}	10		$\rho(10) = 1.000006$	$\tilde{\rho}(10) = 1.000001$
[19] $\delta = 2$	10^{-3}	1	MPC	0.6272687×10^{-2}	0.4428246×10^{-2}
$\alpha = 0.1$			PC	0.6276611×10^{-2}	0.4429159×10^{-2}
$\beta = -0.0025$		10	MPC	0.9905620×10^{-2}	0.6528471×10^{-2}
			PC	0.9911409×10^{-2}	0.6533182×10^{-2}
	10^{-3}	10		$\rho(10) = 1.000605$	$\tilde{\rho}(10) = 1.000464$
	10^{-4}	10		$\rho(10) = 1.000007$	$\tilde{\rho}(10) = 1.000005$
[21] $\delta = 1$	10^{-3}	1	MPC	0.6303023×10^{-3}	0.4600117×10^{-3}
$\alpha = 0.01$			PC	0.6306929×10^{-3}	0.4600706×10^{-3}
$\beta = 0.01$		10	MPC	0.6848886×10^{-3}	0.4712857×10^{-3}
			PC	0.6853077×10^{-3}	0.4714072×10^{-3}
	10^{-3}	10		$\rho(10) = 1.000544$	$\tilde{\rho}(10) = 1.000193$
	10^{-4}	10		$\rho(10) = 1.000006$	$\tilde{\rho}(10) = 1.000002$

Table 7. Known results for the MPC and the PC methods ($E(t)$ is the energy at time level t and c is the velocity).

PDE	Paper	Order	t	ℓ	Results
Sg2	[3, p. 303]	4	7	0.01	$\rho(7) = 3.38$
	[5, p. 277]	3	7	0.01	$\rho(7) = 2.30$
	[6, p. 249]	4	7	0.01	$\rho(7) = 1.21$
Bq	[4, p. 52]	2	36	0.001	0.60×10^{-13} more accurate than PC
			48		0.50×10^{-13}
Sg1	[7, p. 839]	3	[0, 108]	0.001	$L_\infty^{\mathrm{PC}} - L_\infty^{\mathrm{MPC}} \in [0, 0.000012]$
NLS	[9, p. 615]	4	[0, 500]	0.0001	$e \in [0, 10^{-13}]$ ($c = 0.1$)
			[0, 90]		$e \in [0, 3 \times 10^{-14}]$ ($c = 0.5$)

MPC and PC methods from the above papers are given in Table 7, in which [9]

$$e = |E(t) - E(0)|_{\mathrm{PC}} - |E(t) - E(0)|_{\mathrm{MPC}}$$

denotes the difference of the errors of the methods. From Table 7, the following conclusions are obtained:

- In all papers, both the predictor and the corrector methods used were explicit and the method was applied once. This, in contrast to the iterative classical predictor–corrector method, characterizes it as a direct method,
- When the operator D related to the PDE is of second order [3–5, 7], only even orders of D in the recurrence relation should be used. Then this restriction

https://doi.org/10.1017/S1446181113000138 Published online by Cambridge University Press

implies the use of a three-time-level recurrence relation. In general, from the known MPC methods, Proposition 4.1 below is obtained.

- For each individual PDE examined, subject to the stability restrictions for the grid used, in general, the MPC method increases the accuracy achieved. We make the following observations:
  - (i) For fixed time order, this improvement depends on the equation examined (compare with our previous papers [3–7, 9]).
  - (ii) For a fixed equation and time order, the improvement depends on the form of the recurrence relation used and especially on the number of calculations required [6], where, in contrast to our earlier paper [3], the calculation of D^4 is needed. But this limitation cannot be characterized as a limitation of the method, since it is already known that generally in complex physical problems, methods with a great number of calculations should be avoided. However, when the above restrictions are not required, the higher-order in time approximation improves the accuracy [3, 6].
  - (iii) The improvement is significant for values of the time step often used in real-world problems, such as 0.01 and 0.001, while both the MPC and the PC methods tend to have equivalent behaviour as ℓ is refined (compare our earlier paper [9] and the present method, Table 6, when $\ell = 10^{-4}$).

PROPOSITION 4.1. *Consider the initial-value problem*

$$D^p \mathbf{U}(t+\ell) = \mathbf{F}(t), \tag{4.1}$$

where p is a positive integer and $D = \mathrm{diag}\{d/dt\}$ the differential operator related to equation (4.1). Then the MPC method has a recurrence relation of the form $\mathbf{U}(t+\ell) = \mathbf{G}(D^q)$, $q = p, 2p, \ldots$.

COROLLARY 4.1. *The MPC method can be applied to every initial-value problem of the form defined by equation (4.1).*

Finally, as far as the modified Burgers equation is concerned, the MPC method has been applied successfully [8], while its high accuracy is also verified from the comparisons given by Haq et al. [15].

4.2. Two-kink waves Consistent with the physical interpretation given for equation (1.5) in Section 1, this section examines numerically the behaviour of the collision of two single-kink waves with equal moduli of velocities in the following problems, which are part of a more general problem given in Proposition A.2. To avoid enormous solution vectors, the space interval is restricted to [0, 1]. In all experiments the initial condition (1.2) was given by the value $f(x) = u(x, 0)$ with u the theoretical solution (1.5), and the boundary condition (1.3), the time step $\ell = 10^{-3}$ and the space $h = 0.05$ were used.

4.2.1. Problem I Following Proposition A.2(i)(a) with $q_1 = 1$, $q_2 = -1$, a two-kink wave arising from the collision of a single-kink wave with $\delta = 1$, $\beta = 0.1$, $\alpha = 0.1$ and

https://doi.org/10.1017/S1446181113000138 Published online by Cambridge University Press

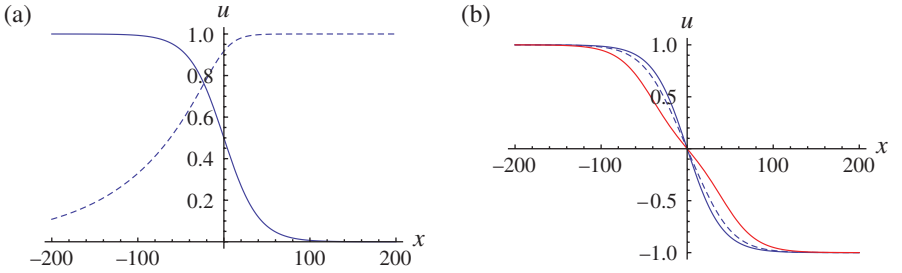

FIGURE 1. Problem I (theoretical solution): two-kink wave when $q_1 = 1$, $q_2 = -1$, $\delta = 1$, $\beta = 0.1$, with $x \in [-200, 200]$. In (a) the full curve shows the individual single-kink wave with $\alpha = 0.1$ and the dashed curve has $\alpha = -0.1$ at $t = 0$. In (b) the resulting two-kink wave is shown at $t = 0$ (full curve), $t = 10$ (dashed curve) and $t = 20$ (red curve). (Colour available online.)

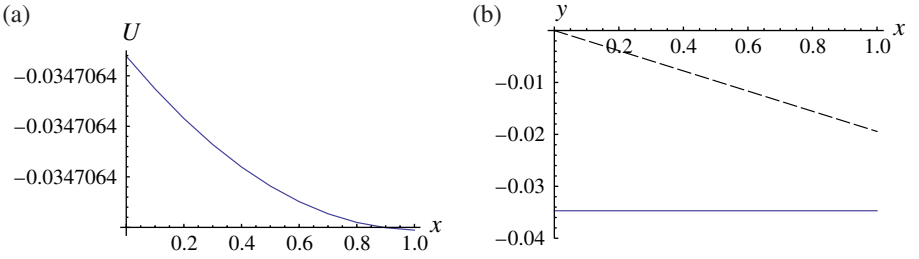

FIGURE 2. Problem I (numerical solution): two-kink wave at $t = 10$. In (a) the curve shows U; in (b) the dashed curve shows u and the full curve U, when the plot range is restricted to $[-0.04, 0]$.

another with $\alpha = -0.1$, moving in the positive (see Figure 1(a), full curve) and negative direction (Figure 1(a), dashed curve) of the x-axis with speed $c = 2.05$ and $c = -2.05$, respectively, is considered. The two-kink wave arising from the collision of these two individual kinks is shown in Figure 1(b) with the full curve at $t = 0$, the dashed curve at $t = 10$ and the red curve at $t = 20$. It is deduced from Figure 1(b) that:

(i) as t increases, the transition point from the homogeneous state -1 to 1 is drawn away from the u-axes;
(ii) the point $(0, 0)$ for all two-kink waves examined is:
   (a) an inflection point;
   (b) the common point of their intersection.

This leads to the conclusion that the resulting two-kink wave has a *quasi* kink behaviour.

Problem I was solved numerically with the mentioned restriction $x \in [0, 1]$. From the results given in Table 8 it is observed that an increment in the errors L_∞ and L_2 occurs as time increases. In Figures 2(a) and 3(a) the curves show U at $t = 10$ and $t = 20$, respectively, while in Figures 2(b) and 3(b) the dashed curve shows u and

https://doi.org/10.1017/S1446181113000138 Published online by Cambridge University Press

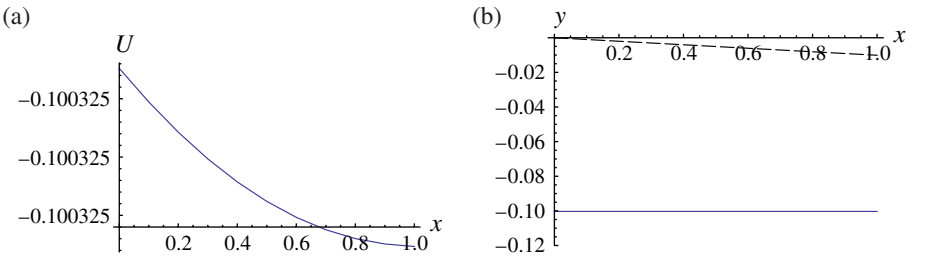

FIGURE 3. Problem I (numerical solution): two-kink wave at $t = 20$. In (a) the curve shows U; in (b) the dashed curve shows u and the full curve U, when the plot range is restricted to $[-0.12, 0]$.

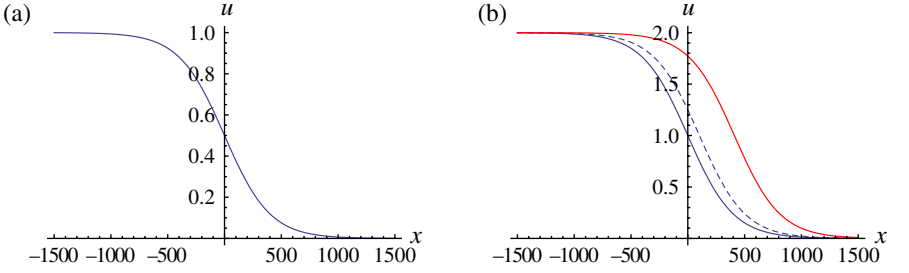

FIGURE 4. Problem II (theoretical solution): two-kink wave when $q_1 = q_2 = 1$, $\delta = 1$, $\alpha = 0.01$, $\beta = 0.001$, with $x \in [-1500, 1500]$. In (a) the curve shows each individual single-kink wave at $t = 0$; in (b) the resulting two-kink wave is shown at $t = 0$ (full curve), $t = 500$ (dashed curve) and $t = 2000$ (red curve). (Colour available online.)

TABLE 8. Two-kink wave. Numerical results with $\delta = 1$, $\ell = 10^{-3}$, $x \in [0, 1]$, $h = 0.05$ and $x_e = 0$.

	Problem I	$(\alpha = 0.1, \beta = 0.1)$	Problem II	$(\alpha = 0.01, \beta = 0.001)$
t	L_∞	L_2	L_∞	L_2
1	0.1379538×10^{-1}	0.8437142×10^{-2}	0.1755659×10^{-2}	0.1012003×10^{-2}
10	0.3462966×10^{-1}	0.2735000×10^{-1}	0.6357037×10^{-2}	0.5477984×10^{-2}
20	0.1000869×10^{0}	0.9996900×10^{-1}	0.1146947×10^{-1}	0.1080929×10^{-1}

the full curve shows U at the relevant time levels. From Figures 2(b) and 3(b), the following conclusions are deduced:

- No visible spurious oscillations of the curve showing U are observed.
- Both the curves showing u and U belong to the fourth quadrant of the coordinate system, while a delay in the propagation of the wave arising from U in comparison with u appears (see Figures 2(b) and 3(b)). This delay increases with time (see Table 8) and has its maximum value at $x = 0$ (x_e in Table 8).
- The transition points are drawn away from the vertical axes more for U than u.

4.2.2. Problem II Finally, following Proposition A.2(ii)(a), a two-kink wave arising from the collision of two single-kink waves with $\delta = 1$, $\alpha = 0.01$ and $\beta = 0.001$ moving in the positive x-axis direction with equal speeds $c = 0.205$ (see Figure 4(a)) is

https://doi.org/10.1017/S1446181113000138 Published online by Cambridge University Press

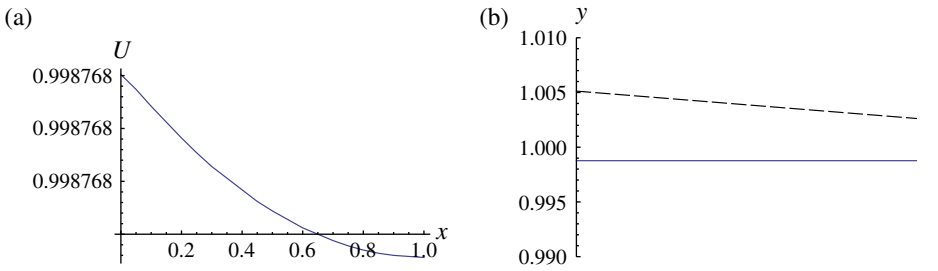

FIGURE 5. Problem II (numerical solution): two-kink wave when $h = 0.05$ and $x \in [0, 1]$ at $t = 10$. In (a) the curve shows U; in (b) the dashed curve shows u and the full curve U, when the plot range is restricted to [0.99, 1.01].

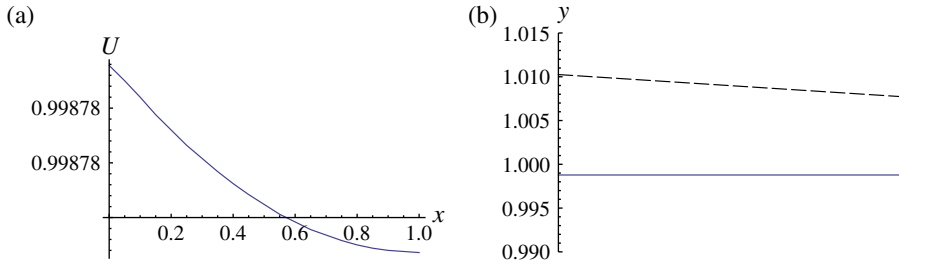

FIGURE 6. Problem II (numerical solution): two-kink wave when $h = 0.05$ and $x \in [0, 1]$ at $t = 20$. In (a) the curve shows U; in (b) the dashed curve shows u and the full curve U, when the plot range is restricted to [0.99, 1.015].

considered. In Figure 4(b), the full curve shows the resulting two-kink wave from the collision of these two individual kinks at $t = 0$, the dashed curve at $t = 500$ and the red curve at $t = 2000$. It is deduced from the latter figure that for the resulting *kink* wave:

(i) as t increases, the transition point approaches the homogeneous state +2, while the transition point to 0 is drawn away from the u-axes;

(ii) it is also moving in the same direction as the two individual kinks.

Problem II was also solved numerically and the results are given in Table 8, while the relevant figures are Figures 5 and 6. The following deductions are made:

- Both the errors L_∞ and L_2 increase with time, but because of the low speed of the individual kinks this increment is slower than the relevant increment in Problem I.
- No visible spurious oscillations of the curve showing U are observed.
- Both the curves showing u and U belong to the first quadrant of the coordinate system.
- A delay in the propagation of the wave arising from U in comparison with u appears (see Figures 5(b) and 6(b)). This delay increases with time (see Table 8) and has its maximum value at $x = 0$ (x_e in Table 8).
- The transition points are drawn away more for U than u.

https://doi.org/10.1017/S1446181113000138 Published online by Cambridge University Press

5. Conclusions

A second-order in time finite-difference scheme using the process of the known modified predictor–corrector method [3–9] has been proposed for the numerical solution of the generalized Burgers–Fisher equation. The computational efficiency of the proposed method has been tested by comparing numerical results arising from experiments with relevant existing results [17, 19, 21, 23] and found to be more accurate. Comparisons with the corresponding classical predictor–corrector method and detailed comments on applicability to other equations are given in Section 4. Also, the behaviour of the collision of two-kink waves with low and high speed have been examined.

The next step for future research on the proposed method would be to investigate its effectiveness in other temporal discretizations, as well as to examine the theoretical criteria for the convergence of the process defined in equation (4.1).

Acknowledgements

The author would like to thank the referees for their valuable comments and suggestions, which have improved the paper.

Appendix A. Single and two-kink waves: theoretical properties

Proposition A.1. *The constant-velocity front of transition from the homogeneous state* 0 *to* 1 *of the solution* u *in equation* (1.4) *has the following properties:*

(i) *For fixed* α *and* β *it approaches the* u*-axes when* δ *increases.*
(ii) *For fixed* β *and* δ *it is drawn away from the* u*-axes when* α *decreases.*
(iii) *For fixed* α *and* δ *it is independent of* β*.*

Proposition A.2. *The constant-velocity front of transition of the solution* u *in equation* (1.5) *depends on the signs of* q_i *and* c_i*,* $i = 1, 2$*. In particular, it has the following properties:*

(i) *If* $q_1 q_2 < 0$ *then:*
  (a) *if* $c_1 c_2 < 0$*, it is from the homogeneous state* -1 *to* 1 *(see Figure* 7(a) *when* $c_1 \neq c_2$ *and Figure* 1(b) *when* $c_1 = c_2$*);*
  (b) *for* $c_1 c_2 > 0$ *with* $c_1 \neq c_2$*, it is from* $-1 + \varepsilon$ *to* $1 - \tilde{\varepsilon}$ *with* $0 < \varepsilon, \tilde{\varepsilon} < 1$ *(see Figure* 7(b)*).*
(ii) *If* $q_1 = q_2 = 1$ *then:*
  (a) *if* $c_1 c_2 > 0$*, it is from* 0 *to* 2 *(see Figures* 8(a) *and* 4(b)*);*
  (b) *for* $c_1 c_2 < 0$ *it is from* $0 + \varepsilon$ *to* $2 - \tilde{\varepsilon}$ *with* $\varepsilon, \tilde{\varepsilon} \in [0, 1]$ *(see Figure* 8(b)*).*
(iii) *If* $q_1 = q_2 = -1$ *then:*
  (a) *if* $c_1 c_2 > 0$*, it is from* -2 *to* 0*;*
  (b) *for* $c_1 c_2 < 0$*, it is from* $-2 + \varepsilon$ *to* $0 - \tilde{\varepsilon}$ *with* $\varepsilon, \tilde{\varepsilon} \in [0, 1]$.

https://doi.org/10.1017/S1446181113000138 Published online by Cambridge University Press

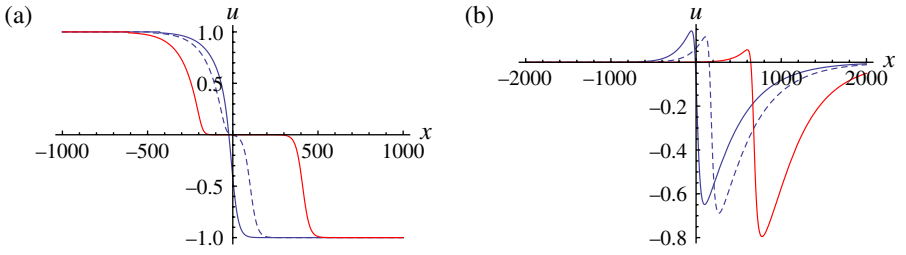

FIGURE 7. Two-kink wave arising from the single kinks k_i, $i = 1, 2$. In (a) k_1: $q_1 = 1$, $\delta = 1$, $\alpha = \beta = 0.1$ ($c_1 = 2.05$), and k_2: $q_2 = -1$, $\delta = 8$, $\alpha = -0.1$, $\beta = 0.01$ ($c = -0.9111$); with $x \in [-1000, 1000]$ at $t = 0$ (full curve), $t = 50$ (dashed curve) and $t = 200$ (red curve). In (b) k_1: $q_1 = 1$, $\delta = 2$, $\alpha = 0.1$, $\beta = 0.01$ ($c = 0.3333$), and k_2: $q_2 = -1$, $\delta = 3$, $\alpha = 0.01$, $\beta = 0.001$ ($c = 0.4025$); with $x \in [-2000, 2000]$ at $t = 0$ (full curve), $t = 500$ (dashed curve) and $t = 2000$ (red curve). (Colour available online.)

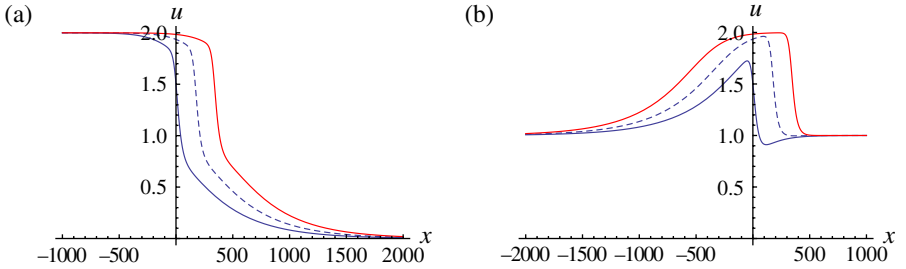

FIGURE 8. Two-kink wave arising from the single kinks k_i, $i = 1, 2$. In (a) k_1: $q_1 = 1$, $\delta = 2$, $\alpha = 0.1$, $\beta = 0.01$ ($c = 0.3333$), and k_2: $q_2 = 1$, $\delta = 3$, $\alpha = 0.01$, $\beta = 0.001$ ($c = 0.4025$); with $x \in [-1000, 2000]$ at $t = 0$ (full curve), $t = 500$ (dashed curve) and $t = 1000$ (red curve). In (b) k_1: $q_1 = 1$, $\delta = 2$, $\alpha = 0.1$, $\beta = 0.01$ ($c = 0.3333$), and k_2: $q_2 = 1$, $\delta = 3$, $\alpha = -0.01$, $\beta = 0.001$ ($c = -0.4025$); with $x \in [-2000, 1000]$ at $t = 0$ (full curve), $t = 500$ (dashed curve) and $t = 1000$ (red curve). (Colour available online.)

References

[1] M. J. Ablowitz and A. Zeppetella, "Explicit solutions of Fisher's equation for a special wave speed", *Bull. Math. Biol.* **41** (1979) 835–840; doi:10.1007/BF02462380.

[2] E. Babolian and J. Saeidian, "Analytic approximate solutions to Burgers, Fisher, Huxley equations and two combined forms of these equations", *Comm. Nonlinear Sci. Numer. Simulation* **14** (2009) 1984–1992; doi:10.1016/j.cnsns.2008.07.019.

[3] A. G. Bratsos, "A modified predictor–corrector scheme for the two-dimensional sine-Gordon equation", *Numer. Algorithms* **43** (2006) 295–308; doi:10.1007/s11075-006-9061-3.

[4] A. G. Bratsos, "A second order numerical scheme for the solution of the one-dimensional Boussinesq equation", *Numer. Algorithms* **46** (2007) 45–58; doi:10.1007/s11075-007-9126-y.

[5] A. G. Bratsos, "A third order numerical scheme for the two-dimensional sine-Gordon equation", *Math. Comput. Simulation* **76** (2007) 271–282; doi:10.1016/j.matcom.2006.11.004.

[6] A. G. Bratsos, "A modified explicit numerical scheme for the two-dimensional sine-Gordon equation", *Int. J. Comput. Math.* **85** (2008) 241–252; doi:10.1080/00207160701417415.

[7] A. G. Bratsos, "A numerical method for the one-dimensional sine-Gordon equation", *Numer. Methods Partial Differential Equations* **24** (2008) 833–844; doi:10.1002/num.20292.

[8] A. G. Bratsos, "A fourth-order numerical scheme for solving the modified Burgers equation", *Comput. Math. Appl.* **60** (2010) 1393–1400; doi:10.1016/j.camwa.2010.06.021.

https://doi.org/10.1017/S1446181113000138 Published online by Cambridge University Press

[9] A. G. Bratsos, "A modified numerical scheme for the cubic Schrödinger equation", *Numer. Methods Partial Differential Equations* **27** (2011) 608–620; doi:10.1002/num.20541.
[10] H. Chen and H. Zhang, "New multiple soliton solutions to the general Burgers–Fisher equation and the Kuramoto–Sivashinsky equation", *Chaos Solitons Fractals* **19** (2004) 71–76; doi:10.1016/S0960-0779(03)00081-X.
[11] S. A. El-Wakil and M. A. Abdou, "Modified extended tanh-function method for solving nonlinear partial differential equations", *Chaos Solitons Fractals* **31** (2007) 1256–1264; doi:10.1016/j.chaos.2005.10.072.
[12] H. Fahmy, "Travelling wave solutions for some time-delayed equations through factorizations", *Chaos Solitons Fractals* **38** (2008) 1209–1216; doi:10.1016/j.chaos.2007.02.007.
[13] R. A. Fisher, "The wave of advance of advantageous genes", *Ann. Eugenics* **7** (1937) 353–369; doi:10.1111/j.1469-1809.1937.tb02153.x.
[14] A. Golbabai and M. Javidi, "A spectral domain decomposition approach for the generalized Burgers–Fisher equation", *Chaos Solitons Fractals* **39** (2009) 385–392; doi:10.1016/j.chaos.2007.04.013.
[15] S. Haq, A. Hussain and M. Uddin, "On the numerical solution of nonlinear Burgers'-type equations using meshless method of lines", *Appl. Math. Comput.* **218** (2012) 6280–6290; doi:10.1016/j.amc.2011.11.106.
[16] H. N. A. Ismail and A. A. Abd Rabboh, "A restrictive Padé approximation for the solution of the generalized Fisher and Burger–Fisher equations", *Appl. Math. Comput.* **154** (2004) 203–210; doi:10.1016/S0096-3003(03)00703-3.
[17] H. N. A. Ismail, K. Raslan and A. A. Abd Rabboh, "Adomian decomposition method for Burger's–Huxley and Burger's–Fisher equations", *Appl. Math. Comput.* **159** (2004) 291–301; doi:10.1016/j.amc.2003.10.050.
[18] M. Javidi, "Spectral collocation method for the solution of the generalized Burger–Fisher equation", *Appl. Math. Comput.* **174** (2006) 345–352; doi:10.1016/j.amc.2005.04.084.
[19] D. Kaya and S. M. El–Sayed, "A numerical simulation and explicit solutions of the generalized Burgers–Fisher equation", *Appl. Math. Comput.* **152** (2004) 403–413; doi:10.1016/S0096-3003(03)00565-4.
[20] A. N. Kolmogorov, I. G. Petrovsky and N. S. Piscounov, "Étude de l'équation de la diffusion avec croisance de la quantité de matiére et son application á un probléme biologique", *Bull. Univ. Moskau Ser. Intl. Sec.* A **1** (1937) 1–25.
[21] M. Moghimi and F. S. A. Hejazi, "Variational iteration method for solving generalized Burger–Fisher and Burger equations", *Chaos Solitons Fractals* **33** (2007) 1756–1761; doi:10.1016/j.chaos.2006.03.031.
[22] M. Sari, "Differential quadrature solutions of the generalized Burgers–Fisher equation with a strong stability preserving high-order time integration", *Math. Comput. Appl.* **16** (2011) 477–486; http://mcajournal.cbu.edu.tr/volume16/vol16no2/v16no2p477.pdf.
[23] M. Sari, G. Gürarslan and I. Dağ, "A compact finite difference method for the solution of the generalized Burgers–Fisher equation", *Numer. Methods Partial Differential Equations* **26** (2010) 125–134; doi:10.1002/num.20421.
[24] M. Sari, G. Gürarslan and A. Zeytinoğlu, "High-order finite difference schemes for the solution of the generalized Burgers–Fisher equation", *Int. J. Numer. Methods Biomed. Eng.* **27** (2011) 1296–1308; doi:10.1002/cnm.1360.
[25] E. H. Twizell, *Computational methods for partial differential equations* (Ellis Horwood, Chichester, 1984).
[26] J. J. Tyson and P. K. Brazhnik, "On traveling wave solutions of Fisher's equation in two spatial dimensions", *SIAM J. Appl. Math.* **60** (1999) 371–391; doi:10.1137/S0036139997325497.
[27] X. Y. Wang, "Exact and explicit solitary wave solutions for the generalised Fisher equation", *Phys. Lett.* A **131** (1988) 277–279; doi:10.1016/0375-9601(88)90027-8.
[28] A.-M. Wazwaz, "The tanh method for generalized forms of nonlinear heat conduction and Burgers–Fisher equations", *Appl. Math. Comput.* **169** (2005) 321–338; doi:10.1016/j.amc.2004.09.054.

[29] A.-M. Wazwaz, "The tanh–coth method for solitons and kink solutions for nonlinear parabolic equations", *Appl. Math. Comput.* **188** (2007) 1467–1475; doi:10.1016/j.amc.2006.11.013.

[30] L. Wazzan, "A modified tanh–coth method for solving the general Burgers–Fisher and the Kuramoto–Sivashinsky equations", *Comm. Nonlinear Sci. Numer. Simulation* **14** (2009) 2642–2652; doi:10.1016/j.cnsns.2008.08.004.

[31] Z.-H. Xu and D.-Q. Xian, "Application of exp-function method to generalized Burgers–Fisher equation", *Acta Math. Appl. Sin. English Ser.* **26** (2010) 669–676; doi:10.1007/s10255-010-0031-0.

[32] T. Zhao, C. Li, Z. Zang and Y. Wu, "Chebyshev–Legendre pseudo-spectral method for the generalised Burgers–Fisher equation", *Appl. Math. Model.* **36** (2012) 1046–1056; doi:10.1016/j.apm.2011.07.059.